УДК 534.6.08

OECD 01.03.AA, 02.03.IU

Sound Source Reconstruction on Flexible Plate backed by a Cavity using Equivalent Source Method

Nagaraja Jade.[1], Venkatesham B.[2*]

[1] Research scholar, Department of Mechanical and Aerospace Engineering, Indian Institute of Technology Hyderabad, Telangana-502585, India

[2] Associate professor, Department of Mechanical and Aerospace Engineering, Indian Institute of Technology Hyderabad, Telangana-502285, India

Abstract

Characterization of sound radiation from thin flexible structures, which encloses sound sources, is required for noise control studies. It involves structural-acoustic coupling between flexible structure and acoustic cavity. The aim of present study is to reconstruct the sound source at uncoupled and coupled frequencies using Equivalent Source Method (ESM) for a rectangular box with the single compliant wall. Data for reconstruction is generated from numerical simulations instead of actual measurements. Effect of the regularization and Signal-to-Noise Ratio (SNR) on the accuracy of reconstruction is discussed. The numerical model is developed to understand the coupling phenomena between structural and acoustic subsystem.

Key words: Equivalent Source Method (ESM), Structural-acoustic coupled system, Regularization, Signal-to-Noise Ratio (SNR).

Воссоздание источника звука на гибкой пластине, поддерживаемой полостью, с использованием метода эквивалентного источника

Нагараджа Джейд. [1]*, Венкатешам Б.* [2*]

[1]*Научный сотрудник, Кафедра машиностроения и аэрокосмической техники, Индийский Технологический институт Хайдарабада, Телангана-502585, Индия*

[2*]*Доцент кафедры машиностроения и аэрокосмической техники Индийского технологического института Хайдарабада, Телангана-502285, Индия*

Аннотация

Для исследования контроля шума необходима характеристика звукового излучения тонких гибких конструкций, которые ограждают источники звука. Это включает конструктивно-акустическую связь между гибкой конструкцией и акустической полостью. Целью настоящего исследования является воссоздание источника звука на несвязанных и связанных частотах с использованием метода эквивалентного источника (ESM) для прямоугольной коробки с одной упругой стенкой. Данные для воссоздания генерируются на основе численного моделирования вместо фактических измерений. Обсуждается влияние регуляризации и соотношения сигнал/шум (SNR) на точность воссоздания. Разработана численная модель для понимания явления связи между конструктивной и акустической подсистемами.

Ключевые слова*: метод эквивалентного источника (ESM), конструктивно-акустическая связанная система, регуляризация, соотношение сигнал/шум (SNR).*

Introduction

Analysis of sound radiation from the flexible structures backed by an air cavity is an interesting problem in enclosure designs, heating, ventilation and air-conditioning (HVAC) problems, engine cover, transformer tank wall, etc. These types of problems involve

*E-mail: venkatesham@iith.ac.in (corresponding author), me12p1002@iith.ac.in

structural-acoustic coupling phenomena between flexible structure and acoustic cavity. Sound radiates efficiently at the coupled frequencies due to structural-acoustic coupling and at uncoupled frequencies due to structural vibrations [1]. It is important to calculate these frequencies to control the noise radiation effectively. Venkatesham et al. studied sound radiation from a rectangular duct with a single and also with four compliant walls [2, 3]. Various direct or indirect (inverse) techniques are available for the characterization of sound radiation. Some of them are sound intensity method, pressure based method, surface contribution method, near-field acoustic holography (NAH) and beamforming [4, 5].

NAH is one of the good inverse techniques to predict the vibro-acoustic properties of the sound source at lower frequencies [6]. It is a method to reconstruct the acoustic pressure, particle velocity and the sound power using sound pressure measured in the 2D holographic plane. NAH method is first presented by Maynard and Williams [7, 8] which has high resolution compared to conventional holography method. To overcome the limitations of planar NAH (since it is confined only to regular shapes), different methods are established for complex shape geometries [9, 10]. Later in 1992, to enhance the conventional holography technique for arbitrarily shaped vibrating surfaces, Bai developed four holography transformation algorithms based on boundary element method (BEM) [11]. Patch NAH methods are established by researchers to overcome the difficulties of implementation of NAH on large structures [12, 13]. Meanwhile, an alternative to BEM technique, equivalent source method is introduced by Sarkissian [14], since BEM requires large computational resources for complex structures. Here, sound field radiated from the noise source is expressed by a set of standard sources like a monopole, dipole or combination as close to the radiating surface. The main advantage of ESM is that the required computational time is much lesser than other NAH methods. Essential benefits of ESM and patch NAH methods are combined and developed new near-field acoustic holography surface decomposition method by Valdivia et al. [15].

As these NAH techniques are the inverse methods, the reconstructed results are ill-posed due to the presence of evanescent waves. Regularization methods are used to overcome the ill-posedness of the problem [16]. Tikhonov regularization is the most commonly used technique for NAH methods [17]. Characterization of flexible structure which encloses the noise source is of great interest to analyze the coupling behavior and sound radiation mechanism. Lin and Pan [18] investigated sound radiation characteristics of box type structures due to structural excitation. Most of the available literature to characterize these types of structures are based on structural excitation.

The objective of the present work is to reconstruct the sound source on a flexible plate backed by a cavity at uncoupled and coupled frequencies using ESM technique. Initially, uncoupled structural, acoustic natural frequencies and coupled frequencies are calculated from finite element analysis, and these results are corroborated with the analytical results available in the literature [2]. As next step, sound pressure radiated from a flexible surface due to acoustic excitation is calculated using FEM-BEM (finite element/boundary element method). Sound pressure (obtained from numerical simulations) data with added white noise are considered for the reconstruction. Tikhonov regularization with generalized cross-validation (GCV) and L-curve parameter selection methods are employed to overcome the ill-posedness problem. Effect of measurement and background noise on the accuracy of reconstruction is studied in terms of the Signal-to-Noise ratio (SNR). Some of the numerical results presented in the current paper are reported in author’s conference paper [19].

The current study will be helpful to understand the effect of parameters such as regularization parameter method and SNR on the accuracy of reconstruction results before performing the experimental measurements. The organization of the paper as follows, Section-1, describes briefly the principle of ESM method for the reconstruction of sound source characteristics, definition of signal-to-noise ratio and calculation of reconstruction error. Section-2 presents the description of numerical simulations and data generation for reconstruction instead of measurement. In section-3, coupled and uncoupled frequencies obtained from numerical and analytical results are discussed. Regularization parameter estimation and reconstruction of sound pressure results are described in section-4. In the last section, the conclusions are presented.

1. Theory

Present section describes the basic principle of Near-Field Acoustic Holography in brief, and methodology of Equivalent Source Method (ESM) based NAH technique. It also presents the definition of Signal-to-Noise Ratio (SNR) and reconstruction error calculation.

1.1. Near-field Acoustic Holography

NAH is an inverse array technique used to reconstruct the acoustic parameters by measuring the sound pressure with an array of microphones, in a parallel and near to the sound source. The principle of the NAH method is shown schematically in the Fig. 1. It depicts the location of the sound source (Z_s), holographic plane (Z_h) and also the reconstruction plane (Z_r). The acoustic parameters can be reconstructed on any plane in-between the source and holographic planes using NAH technique.

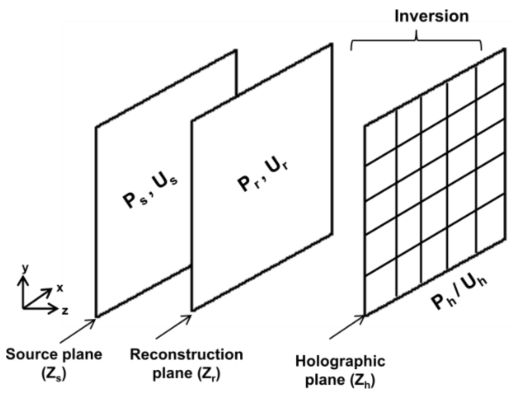

Fig. 1. Schematic diagram of NAH method which depicts source, holographic and reconstruction planes

Sound radiated from the noise source can be measured in terms of sound pressure on any plane with set of measurement points, which is given by [6],

$$\{\boldsymbol{p}_h\}_M = [\mathrm{A}]_{MXN} \{\boldsymbol{q}_s\}_N \tag{1}$$

In Eq. (1), $\boldsymbol{p}_h$ represents the measured sound pressure and $\boldsymbol{q}_s$ is the acoustic source strength. **A** is the transfer matrix (TM) of the dimension of *M*N,* which relates the known pressure to the unknown source strength. *M* is the number of measurement points and *N* is the number of reconstruction points. The calculation of the elements of TM varies for different NAH methods. In ESM method, it can be calculated using free space Green's function, In Inverse boundary element method (IBEM), TM can be obtained using Helmholtz integral equation and for Statistically Optimized NAH (SONAH) method, TM can be formulated using elementary wave functions. As all these NAH methods are an ill-posed problem, regularization is necessary to overcome the ill-posed condition and to reconstruct accurate results. The regularized solution of Eq. (1) is given by,

$$\boldsymbol{q}_s = (\mathbf{A}^H\mathbf{A} + \varepsilon\mathbf{I})^{-1}\mathbf{A}^H\,\boldsymbol{p}_h \tag{2}$$

Here, $\mathbf{I}$ is the identity matrix, H denotes Hermitian transpose, and ε is regularization parameter. Acoustic particle velocity of noise source can also be calculated using the reconstructed sound pressure. Using these reconstructed pressure and particle velocity, active intensity and sound power of the source can be calculated.

1.2. Equivalent source method (ESM)

In ESM method, the sound field is modelled by the distribution of virtual sources such as monopole, dipole or combination of both sources. The acoustic pressure at field point $\mathbf{x}$, based on ESM formulation (in discretized form) is given as follows,

$$p_h(\mathbf{x}_m) = \sum_{n=1}^{N} j\rho ck\, G_{hv}(\mathbf{x}_m, \mathbf{y}_n) q_v(\mathbf{y}_n), \quad m=1, 2,\ldots, \mathrm{M} \tag{3}$$

where, p_h is the measured pressure, q_v is virtual source strength. $\mathbf{x}_m$ and $\mathbf{y}_n$ are position vectors of field point (measurement) and source point, respectively. The G_{hv} is free-space Green's function associated with source point 'n' and field point 'm' and it is given by,

$$\mathrm{G}_{hv}(\mathbf{x}, \mathbf{y}) = \frac{e^{(-jkr)}}{4\pi r}, \tag{4}$$

In Eq. (4), $k = \omega/c$ is the wavenumber, ω is the angular frequency c is the speed of sound, $r = |\mathbf{x} - \mathbf{y}|$ and $j = \sqrt{-1}$. The Eq. (3) can be written in a matrix form as,

$$\mathbf{P}_\mathrm{h} = j\rho\omega\mathbf{G}_{hv}\mathbf{Q}_\mathrm{v} \tag{5}$$

Here, $\mathbf{P}_\mathrm{h}$ represents measured sound pressure vector, $\mathbf{Q}_\mathrm{v}$ represents virtual source strength vector, $\mathbf{G}_{hv}$ is the propagation matrix (transfer matrix), which relates holographic pressure with source volume velocity and ρ is the air density. The unknown source strength can be estimated by inverting Eq. (5) with regularization and solution is as follows,

$$\mathbf{Q}_\mathrm{reg} = \frac{1}{i\rho ck}(\mathbf{G}_{hv}^H\mathbf{G}_{hv} + \varepsilon\mathbf{I})^{-1}\mathbf{G}_{hv}^H\mathbf{P}_h \tag{6}$$

where, $\mathbf{Q}_\mathrm{reg}$ is the regularized estimated source strength, $\mathbf{G}_{hv}^H$ is Hermitian transpose of $\mathbf{G}_{hv}$, ε is the regularization parameter and $\mathbf{I}$ is the identity matrix. Once the source strength is calculated then acoustic parameters can be reconstructed on the surface of actual sound source. The sound pressure on source surface ($\mathbf{P}_s$) can be estimated by using Eq. (7), here, $\mathbf{G}_{sv}$ represents the propagation matrix relating actual source sound pressure to the virtual source strength.

$$\mathbf{P}_s = i\rho\omega\mathbf{G}_{sv}\mathbf{Q}_{reg} \tag{7}$$

1.3. Signal-to-noise ratio (SNR)

It is defined as a ratio of signal power to the noise power. It is also called as dynamic range. It represents the arithmetical difference between the signal and noise levels, in decibels. In other words, it is the ratio of actual signal to the noisy signal, which can be given by the following expression [6],

$$SNR = 20log_{10}\left[\frac{\|P_{signal+noise}-P_{noise}\|}{\|P_{noise}\|}\right] \tag{8}$$

where, $P_{signal+noise}$ is the measured signal with the presence of noise and P_{noise} is the noise signal.

1.4. Signal-to-noise ratio (SNR)

The accuracy of reconstruction of acoustic parameters can be expressed in terms of the reconstruction error. This can be written in general form as [20],

$$\frac{\|P_s-P_{s,\lambda}\ \|_2}{\|P_s\|_2}\ \text{x}\ 100\% \tag{9}$$

where, the vectors P_s and $P_{s,\lambda}$ represents the measured and reconstructed sound pressure, respectively.

2. Numerical simulations

Firstly, the uncoupled structural and acoustical frequencies are calculated using the finite element method. Numerical models for the flexible plate structure and acoustic cavity are shown in Fig.2. For structural analysis, a rectangular plate of the dimension 0.868 m x 1.15 m with 10 gauge (2.5 mm) is modelled and meshed using shell elements. The material properties of the structure are: 71 GPa, Elastic modulus, 2700 kg/m^3, density, and 0.3 Poison's ratio. Simply-supported boundary conditions are applied at edges of the plate and numerical modal analysis is performed using commercial software ANSYS-16 [21]. An acoustic cavity of dimensions 0.868 m x 1.15 m x 1 m is modelled and meshed using SOLID-185 elements. Air properties such as, density of 1.225 kg/m^3, speed of the sound is 340 m/s are applied and acoustic modal analysis is performed. Structural mesh mapped with acoustic mesh and coupled analysis performed using LMS virtual lab-13 [22].

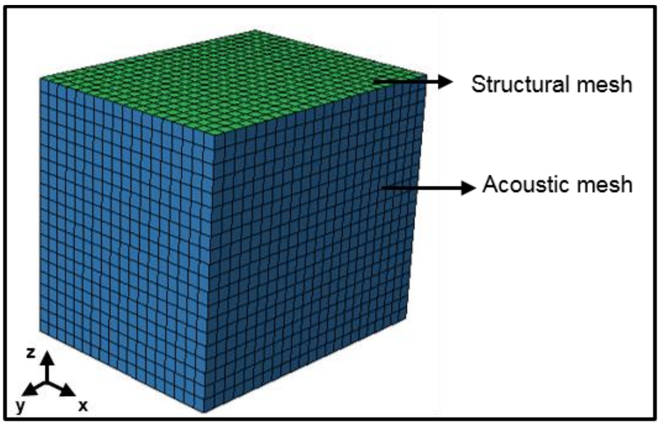

Fig. 2. A numerical model of the structure and an acoustic cavity for coupled analysis.

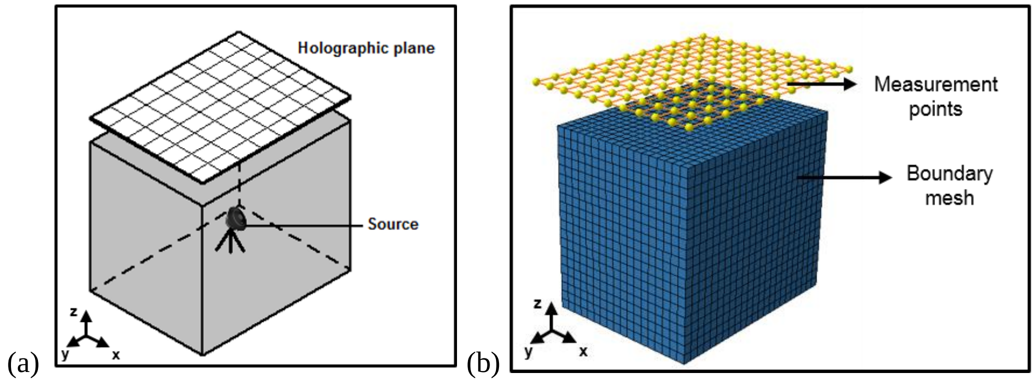

Fig. 3. Radiated sound pressure measurements on the holographic plane:
(a) Schematic (b) Numerical model

Figure 3 shows the schematic and numerical model for radiated sound pressure measurement. FEM-BEM analysis is performed for calculation of radiated sound pressure and power. A monopole source of the strength 0.1 kg/sec^2 is used as an acoustic source for excitation. As the first step, the vibration displacement of the flexible plate due to acoustic excitation is calculated by FEM model. Then vibration displacement is used as input boundary condition for BEM acoustics exterior method for calculation of radiated sound power and pressure. Dimensions of the holographic plane and spacing between measurement points are selected based on the interested frequency range.

3. Structural-acoustic coupled analysis

In this section, discussed numerical and analytical results for uncoupled and coupled natural frequencies of chosen geometry. Effectiveness of coupling is discussed in terms of the coupling transfer factor (TF).

3.1. Uncoupled frequencies

Uncoupled structural and acoustical frequencies calculated from numerical results are compared with analytical results calculated from a mathematical model available in the literature [2]. Table 1 shows the comparison of numerical and analytical results till 200 Hz. Here, f_{sn} represents numerical uncoupled structural frequencies, f_{sa} represents analytical uncoupled structural frequencies. Similarly, f_{an} and f_{aa} represent numerical and analytical uncoupled acoustic frequencies, respectively. It can be observed from Table 1 that uncoupled structural and acoustical modes of numerical results are in good agreement with analytical results.

Table 1
Comparison of numerical and analytical uncoupled structural and acoustical frequencies

Uncoupled structural frequencies						Uncoupled acoustical frequencies		
Mode No.	**f_{sn} (Hz)**	**f_{sa} (Hz)**	**Mode No.**	**f_{sn} (Hz)**	**f_{sa} (Hz)**	**Mode No.**	**f_{an} (Hz)**	**f_{aa} (Hz)**
1	12.69	12.67	11	113.58	114.00	1	147.83	147.83
2	26.48	26.46	12	122.97	123.00	2	170.00	170.00

Uncoupled structural frequencies						Uncoupled acoustical frequencies		
Mode No.	f_{sn} (Hz)	f_{sa} (Hz)	Mode No.	f_{sn} (Hz)	f_{sa} (Hz)	Mode No.	f_{an} (Hz)	f_{aa} (Hz)
3	36.91	36.88	13	133.66	133.71	3	195.85	195.85
4	49.47	49.45	14	145.34	146.18			
5	50.65	50.67	15	146.66	147.21			
6	73.52	73.65	16	147.15	147.50			
7	77.25	77.22	17	169.62	170.49			
8	81.63	81.63	18	173.46	173.57			
9	90.88	91.02	19	186.16	187.56			
10	105.52	105.83	20	196.91	197.78			

3.2. Coupled frequencies

Table 2 shows the comparison of coupled frequencies obtained from numerical simulations with analytically calculated results. They are in good agreement. Here, f_{cn} represents numerical coupled frequencies, f_{ca} represents analytical coupled frequencies. It can be noticed that uncoupled structural frequencies 147.15 Hz, 173.46 Hz and 196.91 Hz are coupled with uncoupled acoustical frequencies 147.83 Hz, 170 Hz and 195.85, respectively. The effective coupled modes can be identified by calculating transfer factor (TF) and it varies from 0 to 1 [2]. TF values close to 1 represents the strong coupling. It can be noticed that uncoupled structural frequency 146.18 Hz is coupled with uncoupled acoustical frequency 147.83 Hz with TF value of 0.887. Similarly, 220.13 Hz structural frequency is coupled with 225.28 Hz acoustic frequency with TF value of 0.78.

Table 2
Comparison of numerical and analytical coupled frequencies

Coupled frequencies					
Mode No.	f_{cn} (Hz)	f_{ca} (Hz)	Mode No.	f_{cn} (Hz)	f_{ca} (Hz)
1	21.99	21.83	13	133.40	133.43
2	26.14	26.12	14	145.03	145.78
3	36.60	36.56	15	146.58	147.12
4	49.73	49.78	16	146.99	147.33
5	50.37	50.39	17	149.34	149.40
6	73.44	73.58	18	169.56	170.42
7	77.34	77.34	19	172.48	172.43
8	81.43	81.41	20	173.50	173.61
9	90.72	90.84	21	186.21	187.61
10	105.43	105.73	22	196.78	196.98
11	113.55	113.99	23	197.01	197.63
12	122.86	122.94	24	201.01	202.61

4. Reconstruction of sound pressure on source surface

In this section, the data generation from numerical simulations for the source reconstruction is described. Regularized parameter selection methods for reconstruction of sound pressure on a flexible surface are described. These reconstructed results have compared with actual sound pressure on source surface obtained from DBEM (direct boundary element method). Effect of SNR on reconstruction error is also discussed.

4.1. Data for the reconstruction

Sound radiated from the flexible surface is estimated in the near-field of the source by a set of virtual microphones. A holographic plane of dimension 1.0 m x 1.3 m with the 11x11 number of measurement points is considered, and it is located at a distance of 0.25m from the flexible surface of the box. The spacing between measuring points along x-direction is 0.1m and along y-direction is 0.13 m. Fig. 4 shows the sound pressure levels at 22 Hz (uncoupled) and 149 Hz (coupled) frequencies with respect to the microphones. It can be noticed that the sound pressure levels at 22 Hz frequency are higher than 149 Hz frequency at all the microphone positions.

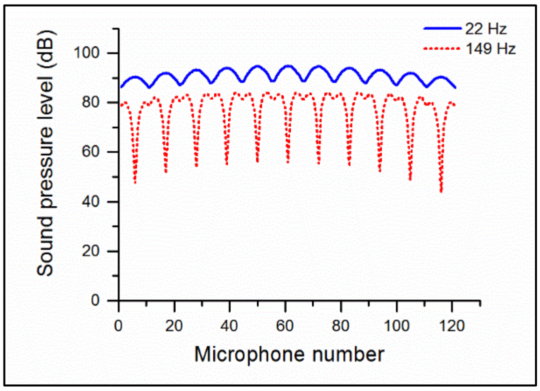

Fig. 4. Radiated sound pressure level on the holographic plane with respect to microphone number at 22 Hz and 149 Hz frequencies.

Sound pressure estimated on the field points is used as input for ESM technique for the reconstruction. In order to create more realistic problems, the perturbation (white noise) is integrated to the pressure signal calculated by the numerical simulations. The added noise incorporates the measurement noise and background noise. Data generation from a numerical simulation with added noise is one of the alternative methods in the absence of measurement array data.

4.2. Radiated sound power calculation

Figure 5 shows the radiated sound power level measured on the holographic plane near the flexible surface of the box structure. It can be observed that sound radiates efficiently at uncoupled structural frequency 22 Hz and acoustic frequency 197 Hz. The sound power levels at these frequencies are 107.34 dB and 123.48 dB, respectively. It can be further noticed from the plot that, there are two peaks around 147 Hz. These closely spaced frequencies are due to the structural-acoustic coupling of uncoupled acoustic mode at 147.83 Hz with the uncoupled structural mode at 147.15 Hz. The split phenomenon occurs due to the energy exchange between acoustic and structural subsystems.

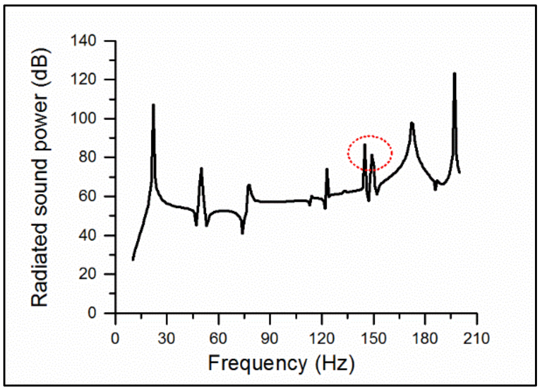

Fig. 5. Sound power level radiated from the flexible surface of the box with respect to frequency.

4.3. Regularization

ESM technique is an ill-posed inverse problem. Therefore regularization is important in order to avoid the amplification of noise presented in the measured pressure. Regularization improves the condition of the inverse matrix. In the present work, Tikhonov regularization with GCV and L-curve parameter selection methods are considered. L-curve plots for the interested frequencies of 22 Hz and 149 Hz are shown in Fig.6 (a) and (b), respectively. These plots show that corner of the L-curve (regularization parameter, ε) occurs at 3.0821e-06 for 22 Hz frequency and 0.003143 for 149 Hz frequency. Similarly, GCV curves for two interested frequencies are shown in Fig. 7(a) and (b). The minimum values of the GCV curve are 2.0269e-04 and 2.4728e-04 for 22 Hz and 149 Hz frequencies, respectively.

4.4. Reconstructed parameters

Sound pressure is reconstructed on the source plane using ESM technique with L-curve and GCV regularization parameter selection methods. Here, total 121 number of monopole sources are chosen in the virtual plane. These are arranged in form of 11 x 11 with the spacing of 0.0868 m in the x-direction and 0.115 m in the y-direction. The retreat distance, (RD, the distance between the actual source plane to the virtual plane) varies from 0.5Δm to 1 Δm for the planar source, where, 'Δ' is the microphone spacing [17]. In the present analysis, RD of 0.0434m and 0.0868m for 22 Hz and 149 Hz frequencies are used to locate the virtual sources, respectively.

(a) (b)

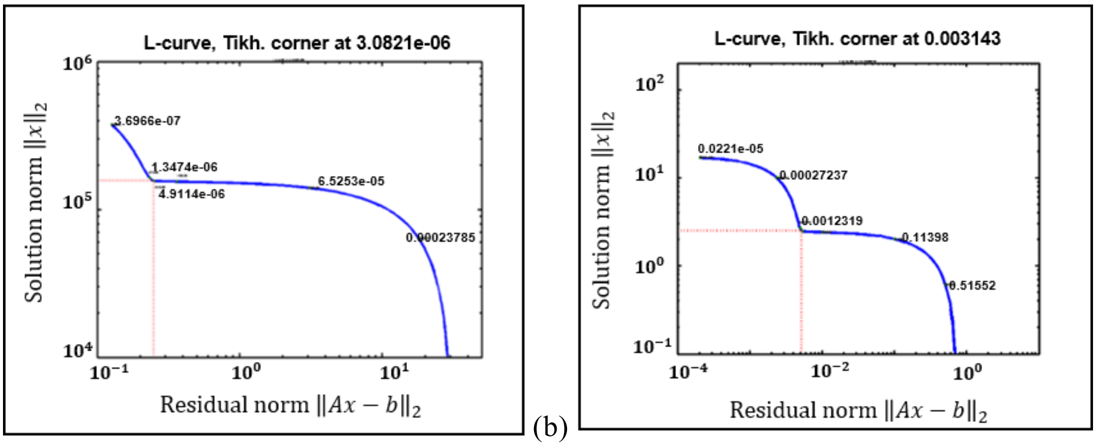

Fig. 6. L-curves for regularization parameter selection at uncoupled and coupled frequencies: (a) 22 Hz (b) 149 Hz.

(a)
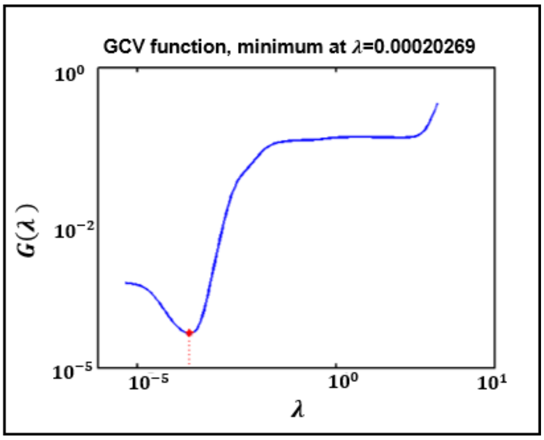

(b)
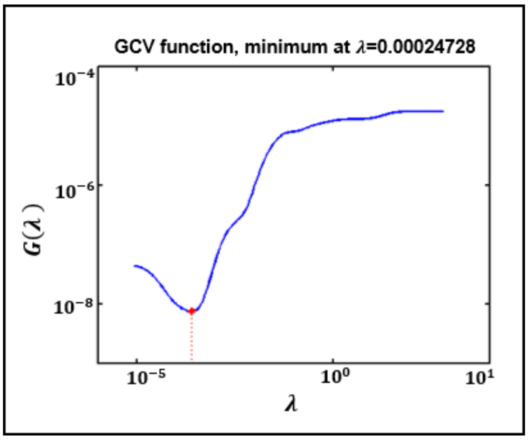

Fig. 7. GCV-curves for regularization parameter selection at uncoupled and coupled frequencies: (a) 22 Hz (b) 149 Hz.

Fig. 8 shows the comparison of reconstructed results with the actual results for 22 Hz and 149 Hz frequencies. It is observed from Fig. 8(a) that, the two regularization parameter selection methods provide reasonable results. However, the magnitude of the pressure obtained using L-curve method is more accurate than the GCV method. Similar behavior is also observed in Fig. 8(b) for 149 Hz frequency. Reconstructed results of the sound pressure on source surface can also be verified by comparing the contour plot of the sound pressure distribution. Fig. 9 shows the contour plots of the actual and reconstructed sound pressure at the frequency of 22 Hz. It can be clearly noticed that reconstructed results are in good match with the actual results.

Figure 10 shows a comparison of actual and reconstructed sound pressure in the form of a contour plot for the coupled frequency of 149 Hz. As it can be observed from the plot, both results are in good agreement. However, there is a small discrepancy between these results due to the coupling effect. Because of the existence of higher-order modes and evanescent wave, the sound radiation pattern varies as keeps moving away from the source surface. Hence, the sound pressure measured on a holographic plane may not have the information of the exponentially decaying waves and which leads to the errors in reconstruction results.

(a)
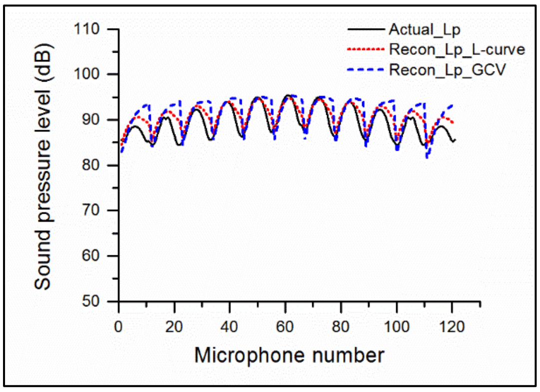

(b)
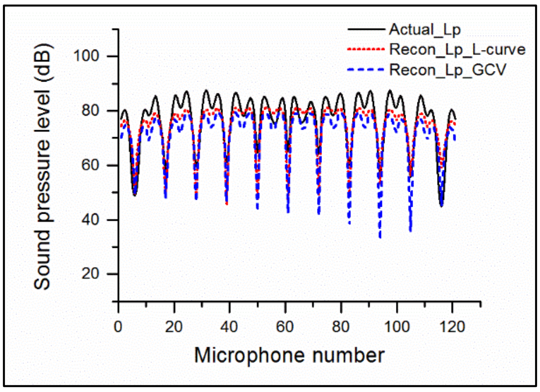

Fig. 8. Comparison of measured and reconstructed sound pressure: (a) Uncoupled frequency 22 Hz, (b) Coupled frequency 149 Hz.

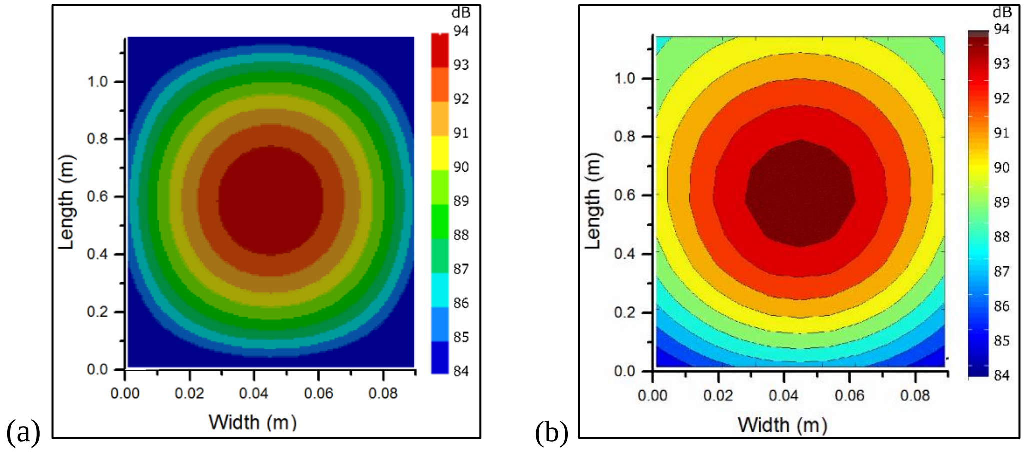

Fig. 9. Comparison of pressure contour plots at uncoupled frequency 22 Hz: (a) Actual, (b) Reconstructed.

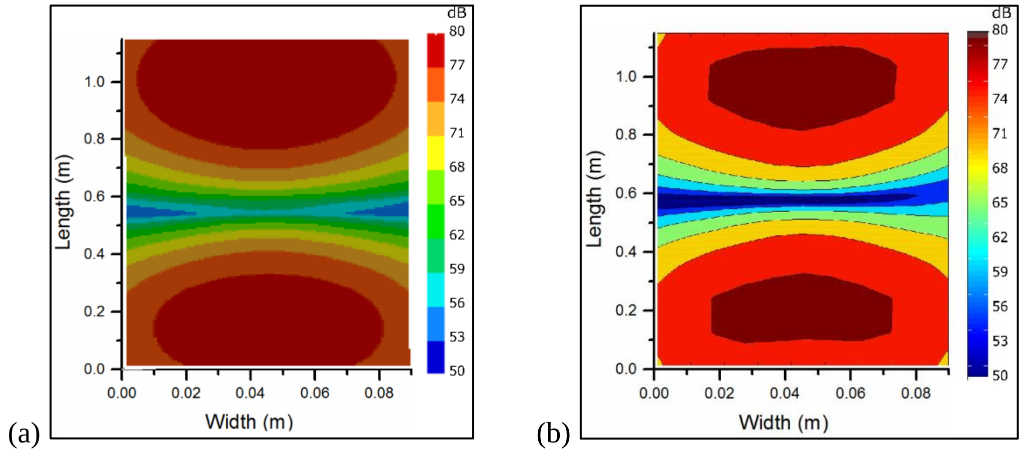

Fig. 10. Comparison of pressure contour plots at uncoupled frequency 149 Hz: (a) Actual, (b) Reconstructed.

4.5. Effect of SNR on reconstruction error

Effect of noise on the accuracy of the reconstruction is studied in terms of the signal-to-noise ratio (dynamic range). Fig. 11 shows the reconstruction error plots as a function of SNR values at uncoupled and coupled frequencies. The different SNR values vary from 25 dB to 50 dB are considered in the intervals of 5 dB. It can be observed that at the uncoupled frequency the reconstruction error decreases uniformly as SNR values increases. However, in case of coupled frequency, the reconstruction error is not uniform. This is because of missing the information of evanescent waves in the measured signal. It is clearly evident from the reconstruction error plots that the SNR values must be high to obtain reconstruction results with less than 15% error.

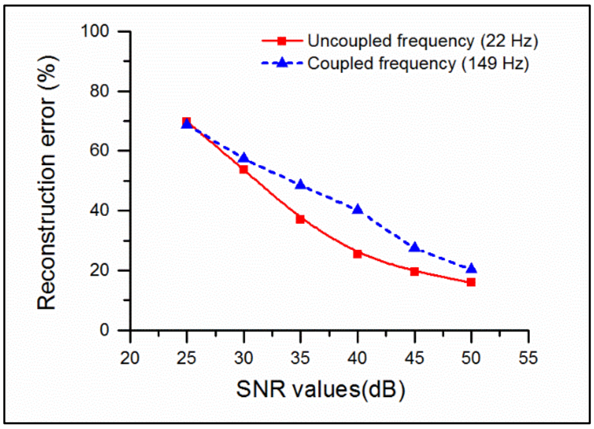

Fig. 11. Maximum reconstruction errors for different signal-to-noise ratio at an uncoupled frequency (22 Hz) and coupled frequency (149 Hz).

Conclusions

In the present paper, as the first step, the uncoupled and coupled natural frequencies are calculated by numerical simulations and corroborated with analytical results. Next, data for reconstruction is generated from predicted sound pressure levels in the near-field of the source. The sound pressure on the flexible surface of the box is reconstructed using equivalent source method. Tikhonov regularization with GCV and L-curve parameter selection methods are employed for solving ill-posed condition. Reconstructed results are compared with actual results at both uncoupled and coupled frequencies. Effect of noise on the accuracy of the reconstruction is studied for different signal to noise ratio (SNR) values. Higher SNR values lead to good accuracy in reconstruction. Based on the regularization studies, it can be concluded that L-curve method is better as compared to GCV method for reconstruction at uncoupled and coupled frequencies.

Acknowledgment

The authors would like to thank Indian Institute of Technology Hyderabad, India for providing the required resources for conducting the current research work.

References

1. Cummings, A. (2001) «Sound transmission through duct walls», Journal of Sound and Vibration, Vol. 239 (4), pp. 731–765.
2. Venkatesham, B., Tiwari, M., Munjal, M.L. (2008) «Analytical prediction of the breakout noise from a rectangular cavity with one compliant wall», Journal of Acoustical Society of America, Vol. 124 (5), pp. 2952–2962.
3. Venkatesham, B., Tiwari, M., Munjal, M.L. (2010) «Analytical prediction of break-out noise from a reactive rectangular plenum with four flexible walls», Journal of Acoustical Society of America, Vol. 128 (4), pp. 1789–1799.
4. Munjal, M.L. Acoustics of ducts and mufflers, 2nd ed., John Wiley & Sons, UK, 2014.
5. Bies, D.A., Hansen, C.H. Engineering noise control: theory and practice, 4th ed., Spon Press, UK and USA, 2009.
6. Bai, M.R., Ih, J.G., Benesty, J. Acoustic array systems: theory, implementation, and application, John Wiley & Sons, Singapore, 2013.

7. Maynard, J.D., Williams, E. G., Lee, Y. (1985) «Near-field acoustic holography: I. Theory of generalized holography and the development of NAH», Journal of Acoustical Society of America, Vol. 78(4), pp. 1395-1413.

8. Williams, E.G., Maynard, J.D., Skudrzyk, E. (1980) «Sound source reconstructions using a microphone array», Journal of Acoustical Society of America, Vol. 68, pp. 340–344.

9. Veronesi, V.A., Maynard, J.D. (1989) «Digital holographic reconstruction of sources with arbitrarily shaped surfaces», Journal of Acoustical Society of America, Vol. 85 (2), pp. 588– 598.

10. Borgiotti, G.V., Sarkissian, A., Williams, E.G., Schuetz, L. (1990) «Conformal generalized near-field acoustic holography for axisymmetric geometries», Journal of Acoustical Society of America, 88 (1), 199–209.

11. Bai, M. R. (1992) «Application of BEM (boundary element method)-based acoustic holography to radiation analysis of sound sources with arbitrarily shaped geometries», Journal of Acoustical Society of America, Vol. 92 (1), pp. 533–549.

12. Saijyou, K. and Yoshikawa, S. (2001) «Reduction methods of the reconstruction error for largescale implementation of near-field acoustical holography», Journal of Acoustical Society of America, Vol. 110 (4), pp. 2007–2023.

13. Williams, E. G., Houston, B. H. and Herdic, P. C. (2003) «Fast Fourier transform and singular value decomposition formulations for patch near-field acoustical holography», Journal of Acoustical Society of America, Vol. 114 (3), pp. 1322–1333.

14. Sarkissian, A. (2004) «Extension of measurement surface in near-field acoustic holography», Journal of the Acoustical Society of America, Vol. 115 (4), pp. 1593–1596.

15. Valdivia, N.P., Williams, E.G., Herdic, P.C., Houston, B. (2012) «Surface decomposition method for near-field acoustic holography», Journal of Acoustical Society of America, Vol. 132 (1), pp. 186–196.

16. Williams, E.G. (2001) «Regularization methods for near-field acoustical holography», Journal of Acoustical Society of America, Vol. 110 (4), pp. 1976-1988.

17. Gomes, J., and Hansen, P.C., (2008) «A study on regularization parameter choice in near-field acoustical holography», Journal of Acoustical Society of America, Vol. 123 (5), pp. 3385-3385.

18. Lin, T.R., Pan, J. (2009) «Sound radiation characteristics of a box-type structure», Journal of Sound and Vibration, Vol. 325(4), pp. 835-851.

19. Nagaraja. J, Venkatesham, B. (2016) «Application of NAH method for the prediction of sound radiation from a flexible box structure» INTER-NOISE and NOISE-CON Congress and Conference Proceedings, Institute of Noise Control Engineering, Vol. 253(4), pp. 3993-3999.

20. Demmel, J. W. Applied Numerical Linear Algebra, University of California, SIAM Publishing Co., California, 1997.

21. ANSYS Engineering Analysis System User's Manual, 2016.

22. LMS International, LMS Virtual Lab Rev 13, User’s Manual, 2013.